

Spectrum Bifurcation in Lattice Massive $SU(2)$ Yang-Mills

Ruggero Ferrari*

Università degli Studi di Milano & INFN, Sez. di Milano

E-mail: ruggero.ferrari@mi.infn.it

We evaluate the spectrum of the $SU(2)$ Massive Yang-Mills (MYM) on the lattice in four dimensions for several points in the β, m^2 parameter space. The region near the Transition Line (TL) is carefully investigated, by starting from the End Point (EP) $\beta \sim 2.2$.

1. The energy gaps are obtained from the “time” correlator of local and gauge invariant operators integrated over the remaining three dimensions.
2. The energy gaps are measured in the isospin $I = 0, 1$ channels according to the global $SU(2)$ symmetry preserved in the deconfined region. Internal spin takes the values $J = 0, 1$.
3. Gaps are found in the channels $I = 1, J = 1$ and $I = 0, J = 0, 1$. Not in the $I = 1, J = 0$ channel.
4. Near the TL a remarkable and new feature is discovered, i.e. a bifurcation of the energy gaps. The onset of the bifurcation occurs much earlier in the $I = 1, J = 1$ channel with distinct properties: the lower gap follows the bare value $|m|$ with a vanishing weight in the Källén-Lehmann representation while the higher gap rises rapidly to a almost constant value and it is dominant for $m^2 \simeq m_c^2$.

QCD-TNT-III-From quarks and gluons to hadronic matter: A bridge too far?,

2-6 September, 2013

European Centre for Theoretical Studies in Nuclear Physics and Related Areas (ECT), Villazzano, Trento (Italy)*

*Speaker.

1. Introduction

A consistent theory of massive $SU(2)$ Yang-Mills theory has been recently proposed [1], [2], where the subtraction procedure of the infinities is performed according a Local Functional Equation (LFE) introduced in Ref. [3]. The mass M appears in a term *à la* Stückelberg

$$S_{YM} + M^2 \int d^4x \text{Tr} \left\{ \left[gA_\mu - i\Omega \partial_\mu \Omega^\dagger \right]^2 \right\}, \quad \Omega \in SU(2). \quad (1.1)$$

The theory can be used in a loop expansion at low energy. High energy processes enter in the realm of the non-perturbative regime, since no Higgs is present in the tree level action. A lattice formulation would be very interesting in order to test the predictions of the continuum whenever is possible. Moreover an obvious question arises whether the spectrum of the lattice theory contains a Higgs-like scalar, that has been excluded at the tree level in eq. (1.1).

A very interesting candidate is the following action on the cubic lattice of size $N \equiv L^4$ with sites x and links μ (see Ref. [4])

$$S_L = \frac{\beta}{2} \Re e \sum_{\square} \text{Tr} \{ 1 - U_{\square} \} + \frac{\beta}{2} m^2 \Re e \sum_{x\mu} \text{Tr} \left\{ 1 - \Omega(x)^\dagger U(x, \mu) \Omega(x + \mu) \right\}, \quad (1.2)$$

where the sum over the plaquette is the Wilson action and $U(x, \mu), \Omega(x) \in SU(2)$. In fact in the naive limit of zero lattice spacing a one gets the action in (1.1) with $M^2 = a^{-2} m^2$.

The action (1.2) is invariant under the **local-left** transformations $g_L(x) \in SU(2)_L$ and the **global-right** transformations $g_R \in SU(2)_R$ (see Ref. [4])

$${}_{SU(2)_L} \left\{ \begin{array}{l} \Omega'(x) = g_L(x) \Omega(x) \\ U'(x, \mu) = g_L(x) U(x, \mu) g_L^\dagger(x + \mu) \end{array} \right., \quad {}_{SU(2)_R} \left\{ \begin{array}{l} \Omega'(x) = \Omega(x) g_R^\dagger \\ U'(x, \mu) = U(x, \mu) \end{array} \right. . \quad (1.3)$$

We would like to stress the importance of this invariance property, in particular because in the **nonrenormalizable** continuum Minkowskean theory it is the starting point for the **removal** of the ultraviolet divergences of the loop expansion. In fact the invariance of the path integral measure ensures the validity of the LFE for the generating functionals [3].

The above lattice model has been studied earlier as a Higgs model where the radius of the field is *frozen*. Most of the work has been concerned about the nature of the change of phase across the TL [5] -[12]. But, once a continuum theory has been shown to exist [1], [2], then the model can be used as lattice regularization of the MYM and the dynamics can be consistently investigated [4].

This work presents a survey of the spectrum in the deconfined region. The region close the TL is investigated in finer details, since it has complex features that can be relevant for phenomenology in the continuum limit.

All the channels are investigated: $(I = 0, 1)$ $(J = 0, 1)$, but only the results of the simulation are given. The phenomenological interpretation is left to a future work.

The features of the spectrum are remarkable: i) there is no correlation in the $(I = 1, J = 0)$ channel: in all others channels there are energy gaps; ii) for m away from the critical value $m_c(\beta)$ the fit requires a single exponential; iii) for m near the TL there is a bifurcation of the energy gaps, with earlier onset in the $(I = 1, J = 1)$ channel than in $(I = 0, J = 0, 1)$ for decreasing m ; iv) in the Källén-Lehmann representation the weight of lower gap vanishes while that of the higher becomes dominant for $m \rightarrow m_c$.

2. Features of the Lattice Model

The statistics is performed by using the partition function

$$Z[\beta, m^2, N] = \sum_{\{U, \Omega\}} e^{-S_L}. \quad (2.1)$$

In principle the integration over $\Omega(x)$ is redundant, since by a change of variables ($U_\Omega(x, \mu) := \Omega(x)^\dagger U(x, \mu) \Omega(x + \mu)$) we can factor out the volume of the group. $Z[\beta, m^2, N]$ becomes

$$\left[\sum_{\{\Omega\}} \right] \sum_{\{U\}} \exp -\beta \left(\frac{1}{2} \Re e \sum_{\square} \text{Tr}\{1 - U_{\square}\} + \frac{1}{2} m^2 \Re e \sum_{x\mu} \text{Tr}\{1 - U(x, \mu)\} \right). \quad (2.2)$$

In eq. (2.2) the integration over Ω has disappeared; consequently Ω in eq. (5.1) does not describe any physical degree of freedom. In that respect we are at variance with other approaches to the same action (1.2) as in [5]-[12], where the field Ω is thought of as a Higgs field with frozen length. In eq. (5.1) we force the integration over the gauge orbit U_Ω by means of the explicit sum over Ω . In doing this we gain an interesting theoretical setup of the model; in practice, our formalism is manifestly gauge invariant (Section 3). Moreover by forcing the integration over the gauge orbit U_Ω we get results which are less noisy than those obtained by using only the integration over the link variables in (2.2).

It is well established that a Transition Line (TL) exists with end point at $\beta \simeq 2.2$ where energy and order parameter ($D = 4$) (see Ref [4])

$$\mathfrak{e} = \frac{1}{DN\beta} \frac{\partial}{\partial m^2} \ln Z = \frac{1}{2ND} \left\langle \Re e \sum_{x\mu} \text{Tr}\{\Omega^\dagger(x) U(x, \mu) \Omega(x + \mu)\} \right\rangle \quad (2.3)$$

have an inflection point becoming steeper by increasing β . See Fig. 1.

3. Gauge invariant Fields

We study the two-point functions which can provide some information on the spectrum. The gauge invariant fields are very useful (τ_a are the Pauli matrices).

$$C(x, \mu) := \Omega^\dagger(x) U(x, \mu) \Omega(x + \mu) = C_0(x, \mu) + i\tau_a C_a(x, \mu). \quad (3.1)$$

By construction

$$C(x, \mu) \in SU(2). \quad (3.2)$$

$C(x, \mu)$ is invariant under **local-left transformations** (1.3), while under the global-right transformations it has $I = 0$ (C_0) and $I = 1$ (C_a) components (I is the isospin). One has

$$C_0(x, \mu)^2 + \sum_{a=1,3} C_a(x, \mu)^2 = 1. \quad (3.3)$$

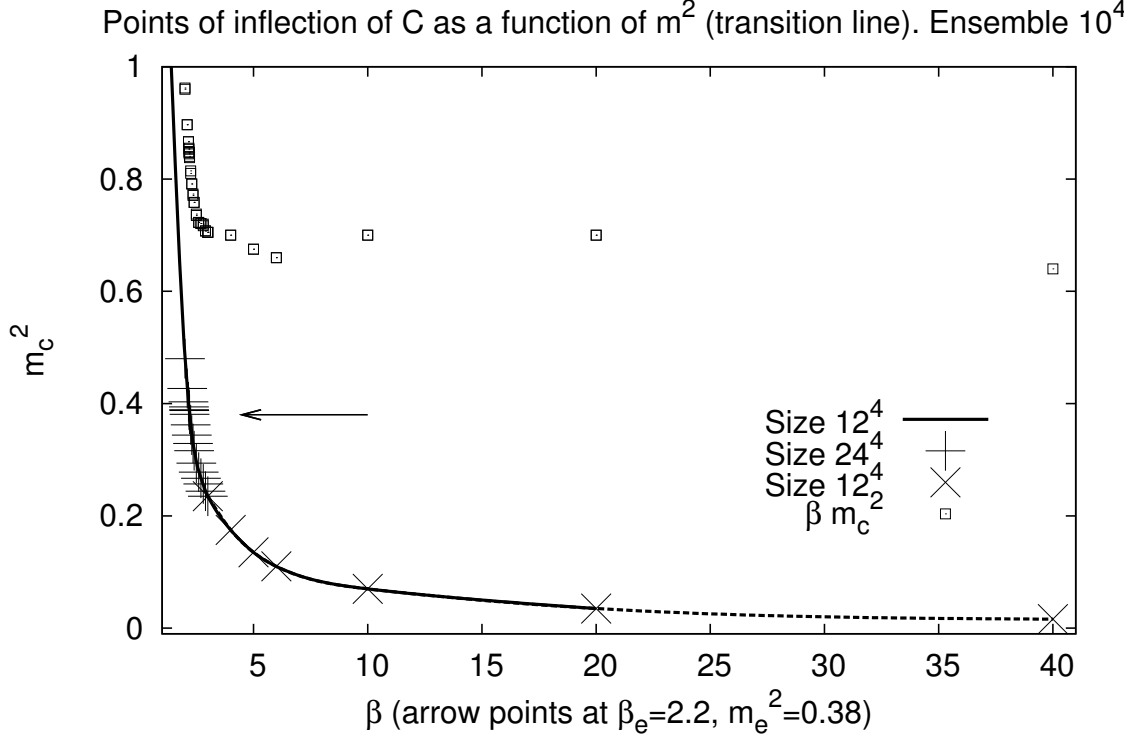


Figure 1: The transition line. The arrow marks the position of the end point. In the figure data from previous analysis have been used and the statistical errors are not displayed since they are too small to be shown.

4. Correlators: General Properties

In the [deconfined](#) region we expect the global-right symmetry to be implemented and therefore

$$\begin{aligned} \langle C_a(x, \mu) \rangle &= 0 \\ \langle C_a(x, \mu) C_b(y, \nu) \rangle &= 0, \quad \text{if } a \neq b. \end{aligned} \quad (4.1)$$

The equations in (4.1) are satisfied by the numerical simulations to a reasonable level of accuracy.

5. Correlators: Energy Gaps

Consider the two-point function of the **zero** -three-momentum operator

$$C_j(t, \mu) = \frac{1}{L^3} \sum_{x_1, x_2, x_3} C_j(x_1, x_2, x_3, x_4, \mu)|_{x_4=t}, \quad j = 0, 1, 2, 3. \quad (5.1)$$

Then we evaluate the connected correlator

$$C_{jj', \mu\nu}(t) = \frac{1}{L} \sum_{t_0=1, L} \langle C_j(t+t_0, \mu) C_{j'}(t_0, \nu) \rangle_C. \quad (5.2)$$

The correlator is zero unless $j = j'$ and $\mu = \nu$. The spin one- and zero- amplitudes V and S are extracted by using the relation

$$C_{jj,\mu\nu}(t) = V_{jj}(\delta_{\mu\nu} - \delta_{\mu 4}\delta_{\nu 4}) + S_{jj}\delta_{\mu 4}\delta_{\nu 4}. \quad (5.3)$$

Very good fit of the data is obtained by using the function

$$g(t) = \frac{1}{2}(f(t) + f(L-t))$$

$$f(t) = b_1 e^{-m_1 t} + b_2 e^{-m_2 t}. \quad (5.4)$$

Two exponentials are needed only for $m \simeq m_c$, as we will illustrate shortly. Otherwise one single exponential is enough for the fit. For comparison the $\beta = 1.5$ single exponential is shown with the $\beta = 3$ two exponentials in Fig. 2 and 3.

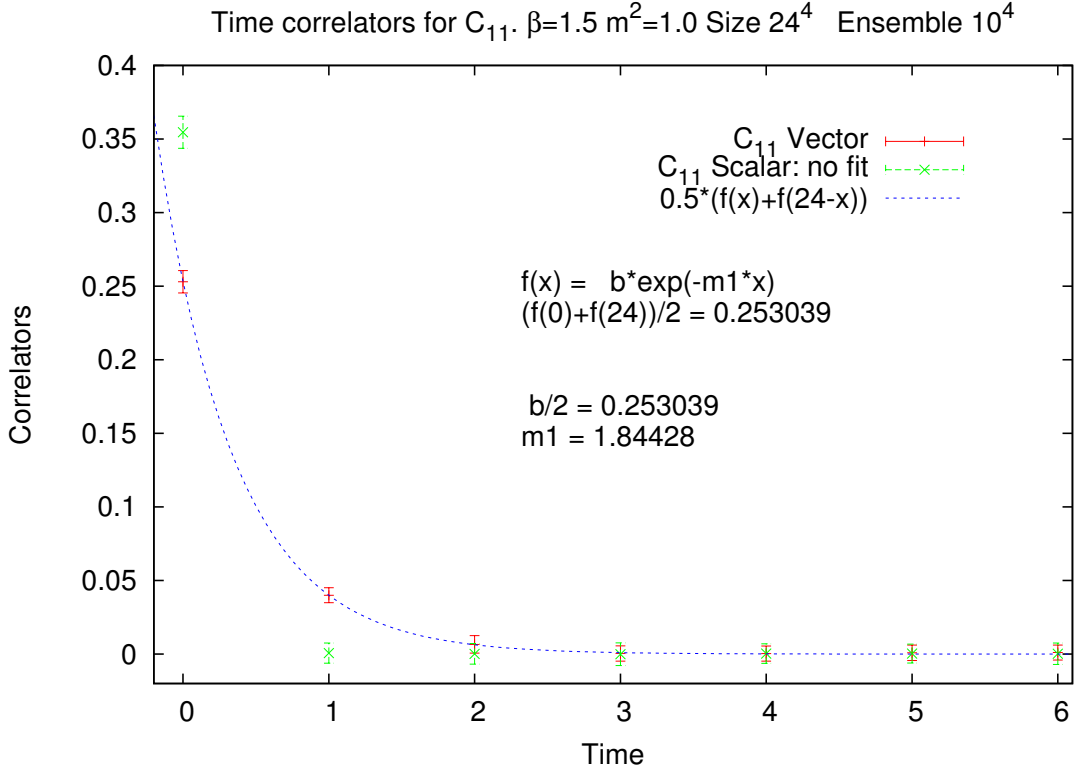


Figure 2: A time correlator in the isovector channel where a single exponential is used. The mass m^2 is close to the TL at $m_{TL}^2 \sim 0.9$.

6. The Spectrum for $\beta = 1.5$

For comparison we show the result of the simulation at $\beta = 1.5$, i.e. close to the EP but still in the region of a single phase. We explore all three channels $I = 1, J = 1$ and $I = 0, J = 0, 1$. Fig. 2 shows that the single exponential fit is good. Fig. 4 and Fig. 5 give the spectrum in each channel. The $I = 1, J = 1$ is the candidate for the vector meson: its mass m_1 follows the bare curve $\sqrt{m^2}$.

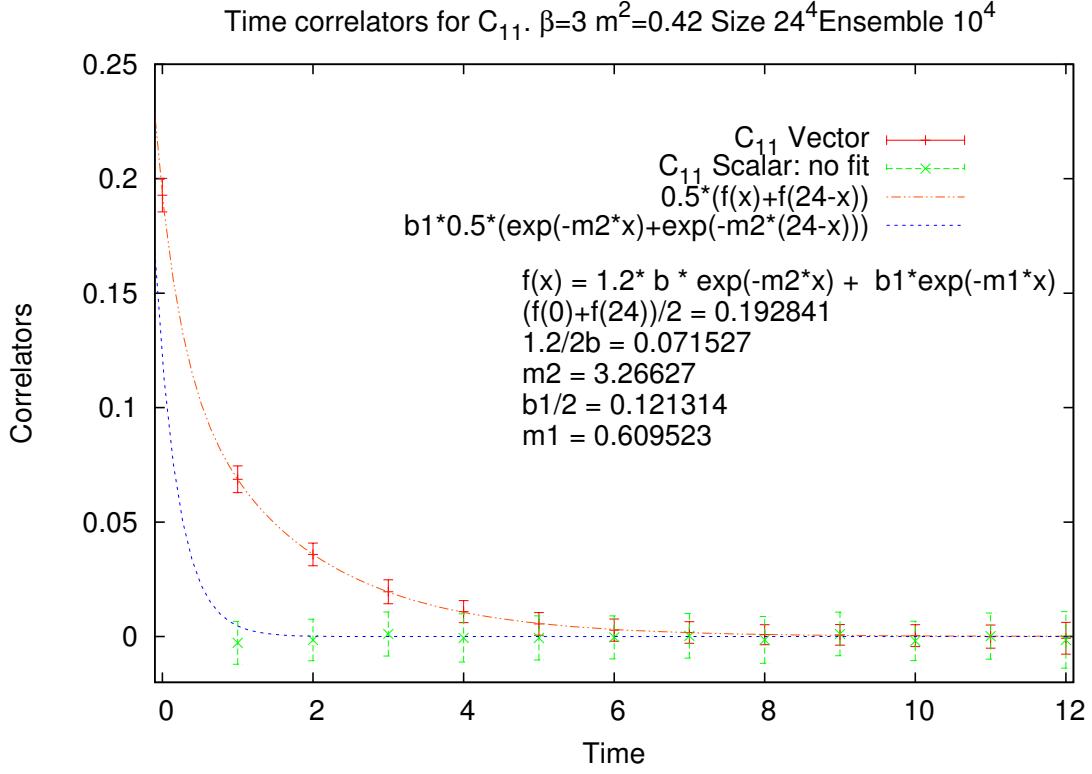


Figure 3: A time correlator in the isovector channel where two exponentials are used. The mass m^2 is close to the TL at $m_c^2 \sim 0.231$. The figure shows the contribution of the large energy gap.

7. The Spectrum for $\beta = 10$

For β above the end point the fit with two exponentials becomes necessary as m^2 approaches m_c^2 . Typically (clearer in the isovector channel) there is a bifurcation point where one gap follows the bare value m and the other is very large. A series of Figures illustrates the phenomenon: Fig. 6 for $I = 1, J = 1$, Fig. 7 for $I = 0, J = 0$, Fig. 8 for $I = 0, J = 1$. By m^2 approaching m_c^2 the weight of the large gap becomes dominant as shown in Fig. 9 for $I = 1, J = 1$, Fig. 10 for $I = 0, J = 0$ and Fig. 11 for $I = 0, J = 1$. These features are once more a distinct sign of the transition from the unconfined to the confined phase. It is particularly clear in the isovector-vector channel (gauge bosons). By approaching the TL the weight of the lower gap vanishes while the large gap become dominant. By crossing the TL the lower gap disappears and the correlation vanishes. This process occurs at the TL, that tends asymptotically to zero for $\beta \rightarrow \infty$. Thus in the limit the mass of the gauge bosons acquires more and more lower values before disappearance.

8. Conclusions

Let us summarize the results of the lattice simulation of the lattice MYM regarding the spectrum.

- i) No correlation in the $I = 1, J = 0$ channel

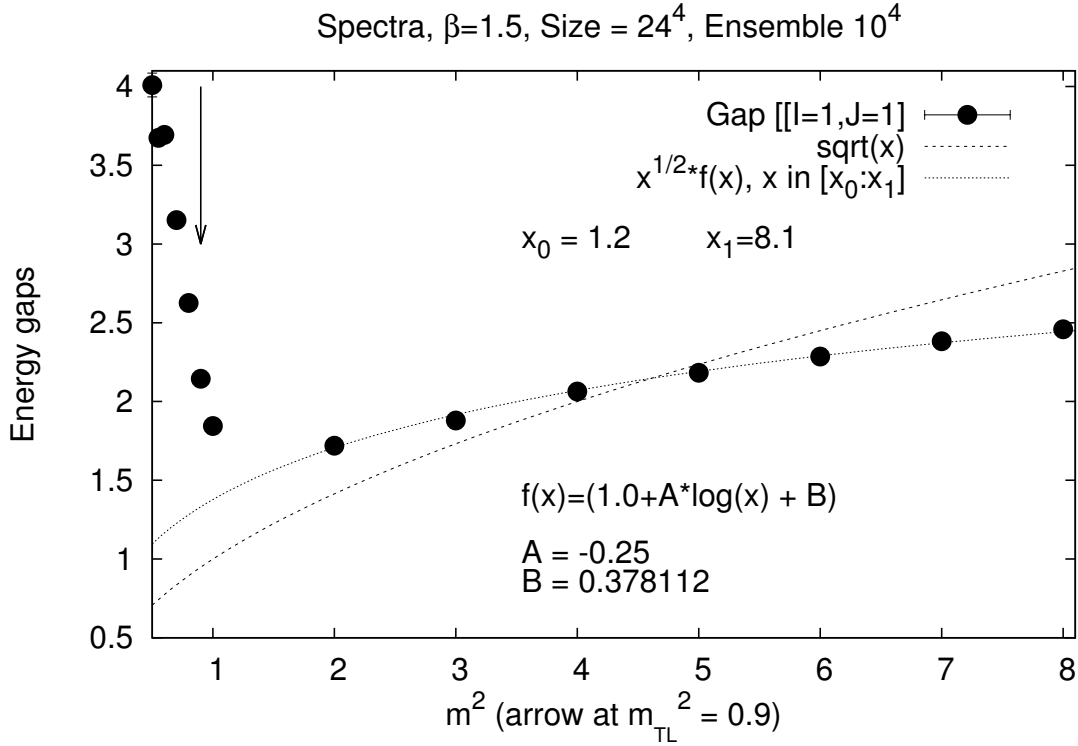


Figure 4: Mass spectrum of the gauge vector meson for $\beta = 1.5$.

- ii) Single exponential fit of correlators for $\beta < 2.2$ and for $m^2 \gg m_c^2$. Bifurcation to two exponential fit for $m^2 \simeq m_c^2$.
- iii) The $I = 1, J = 1$ gap follows close the bare value m .
- iv) In the Källén-Lehmann representation the weight of the lower gap vanishes for $m \rightarrow m_c$
- v) while in the same limit the higher gap dominates.

Further results on the spectrum has appeared in [13].

Outlook:

1. Study the properties of the TL,
2. Understand the deviation of the vector meson mass from the bare value,
3. Examine the origin of the larger gap present after the bifurcation.

References

- [1] D. Bettinelli, R. Ferrari and A. Quadri, "A Massive Yang-Mills Theory based on the Nonlinearly Realized Gauge Group," Phys. Rev. D **77** (2008) 045021 [arXiv:0705.2339 [hep-th]].
- [2] D. Bettinelli, R. Ferrari and A. Quadri, "One-loop Self-energy and Counterterms in a Massive Yang-Mills Theory based on the Nonlinearly Realized Gauge Group," Phys. Rev. D **77**, 105012 (2008) [arXiv:0709.0644 [hep-th]].

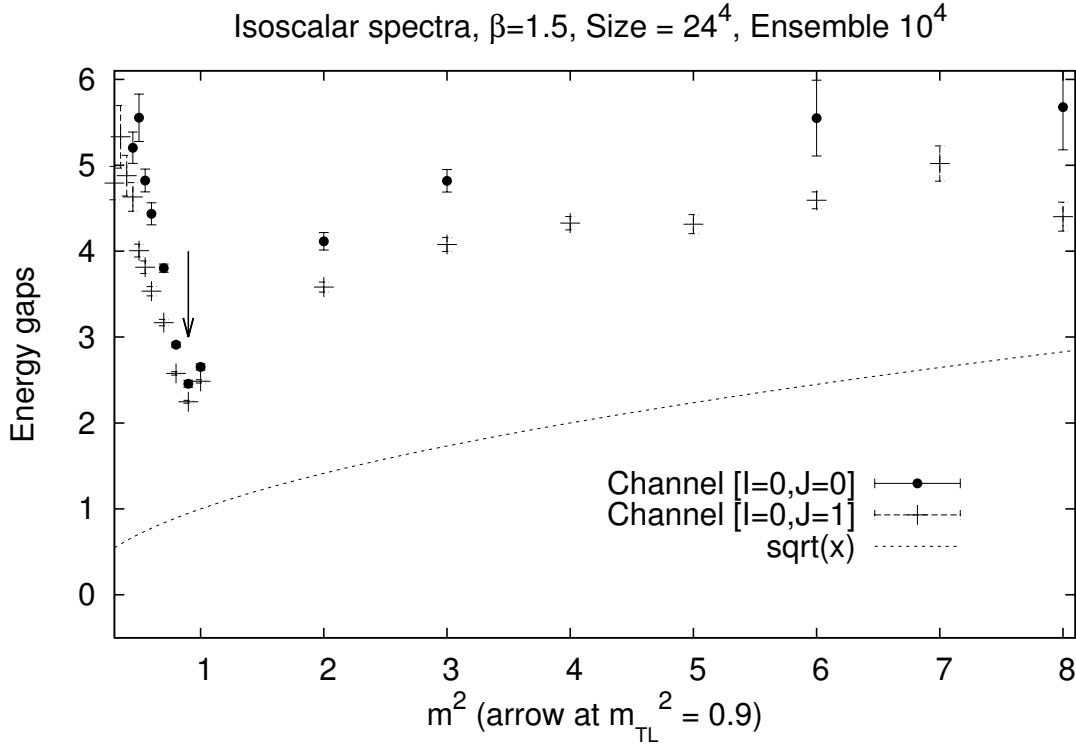


Figure 5: Mass spectrum in the isoscalar channels ($J = 0, 1$) for $\beta = 1.5$.

- [3] R. Ferrari, “Endowing the nonlinear sigma model with a flat connection structure: A way to renormalization,” *JHEP* **0508**, 048 (2005) [arXiv:hep-th/0504023].
- [4] R. Ferrari, “On the Phase Diagram of Massive Yang-Mills,” *Acta Phys. Polon. B* **43** (2012) 1965 [arXiv:1112.2982 [hep-lat].
- [5] E. H. Fradkin and S. H. Shenker, “Phase Diagrams Of Lattice Gauge Theories With Higgs Fields,” *Phys. Rev. D* **19**, 3682 (1979).
- [6] J. Jersak, C. B. Lang, T. Neuhaus, G. Vones, “Properties Of Phase Transitions Of The Lattice SU(2) Higgs Model,” *Phys. Rev.* **D32**, 2761 (1985).
- [7] H. G. Evertz, J. Jersak, C. B. Lang, T. Neuhaus, “Su(2) Higgs Boson And Vector Boson Masses On The Lattice,” *Phys. Lett.* **B171**, 271 (1986).
- [8] H. G. Evertz, V. Grosch, J. Jersak, H. A. Kastrup, T. Neuhaus, D. P. Landau, J. L. Xu, “Monte Carlo Analysis Of Gauge Invariant 2 Point Functions In An Su(2) Higgs Model,” *Phys. Lett.* **B175**, 335 (1986).
- [9] I. Campos, “On the SU(2)-Higgs phase transition,” *Nucl. Phys. B* **514**, 336 (1998) [arXiv:hep-lat/9706020].
- [10] J. Greensite and S. Olejnik, “Vortices, symmetry breaking, and temporary confinement in SU(2) gauge-Higgs theory,” *Phys. Rev. D* **74**, 014502 (2006) [arXiv:hep-lat/0603024].

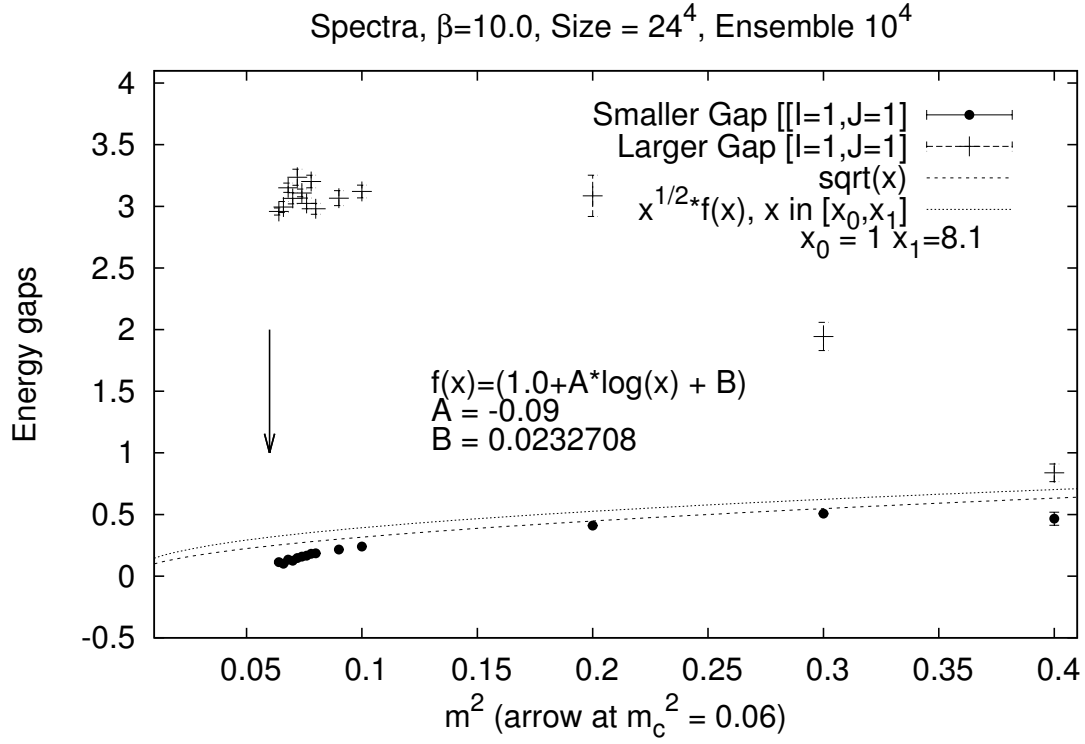


Figure 6: Mass spectrum in the isovector channel ($J = 1$) for $\beta = 10$.

- [11] W. Caudy and J. Greensite, “On the Ambiguity of Spontaneously Broken Gauge Symmetry,” Phys. Rev. D **78**, 025018 (2008) [arXiv:0712.0999 [hep-lat]].
- [12] C. Bonati, G. Cossu, M. D’Elia and A. Di Giacomo, “Phase diagram of the lattice SU(2) Higgs model,” Nucl. Phys. B **828**, 390 (2010) [arXiv:0911.1721 [hep-lat]].
- [13] R. Ferrari, “On the Spectrum of Lattice Massive SU(2) Yang-Mills,” Acta Phys. Polon. B **44**, no. 9, 1871 (2013) [arXiv:1308.1111 [hep-ph]].

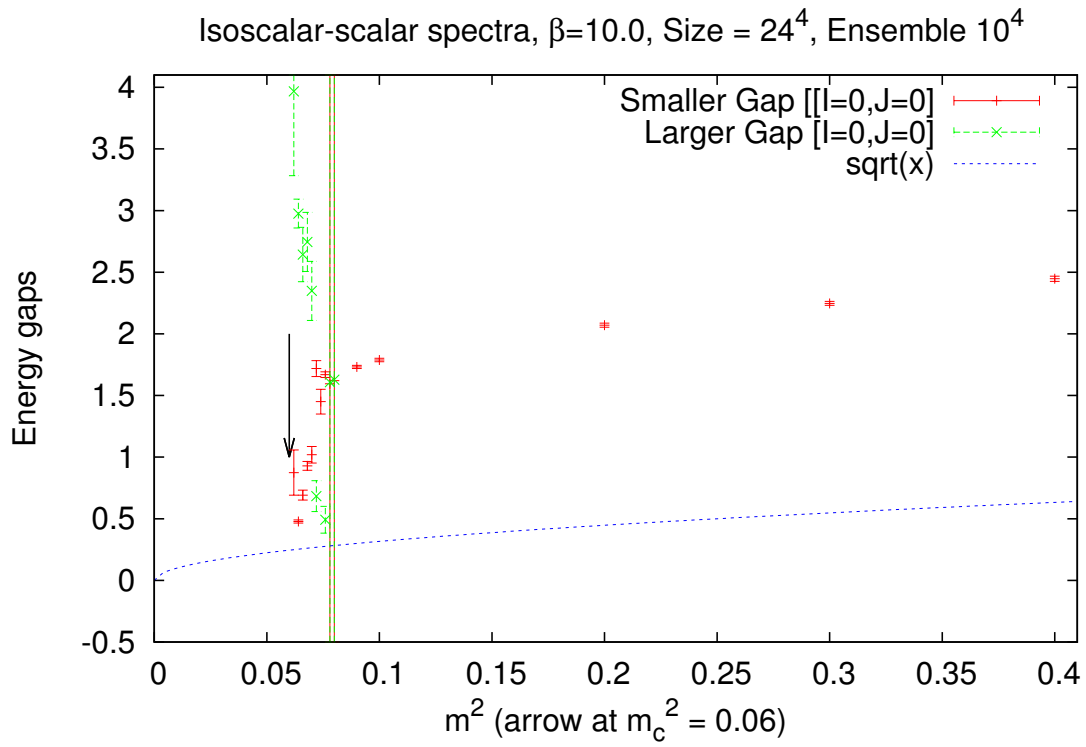


Figure 7: Mass spectrum in the isoscalar channel ($J = 0$) for $\beta = 10$.

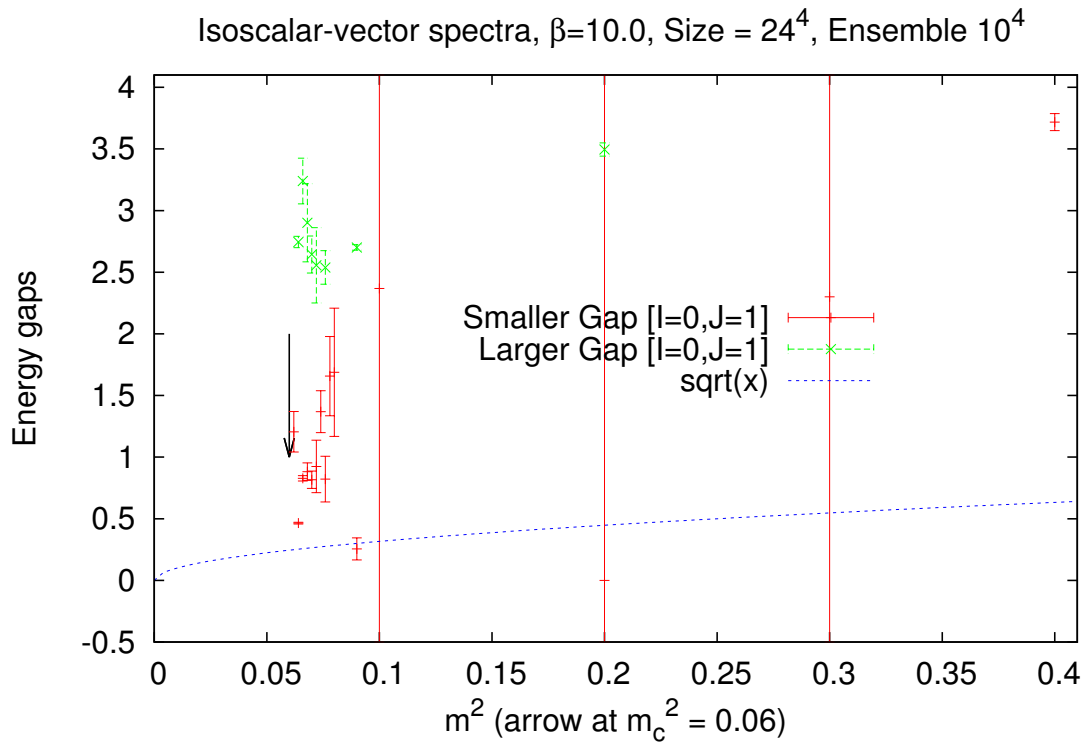


Figure 8: Mass spectrum in the isoscalar channel ($J = 1$) for $\beta = 10$.

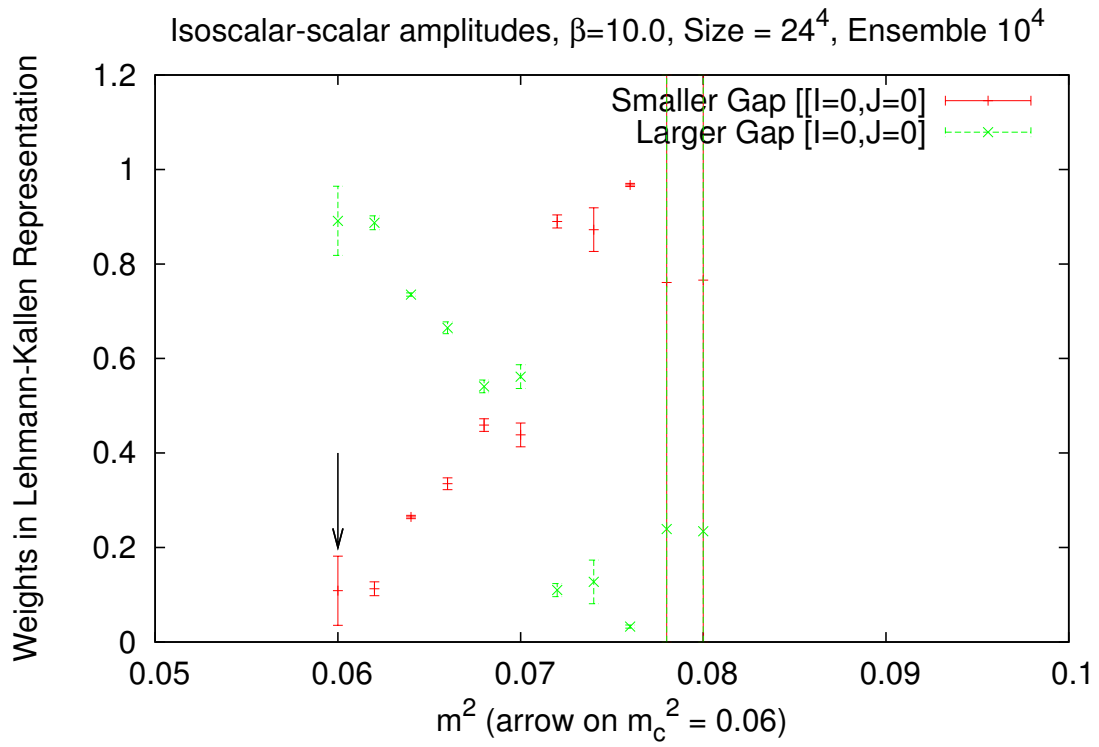


Figure 10: Weights in the isoscalar channel ($J = 0$) for $\beta = 10$.

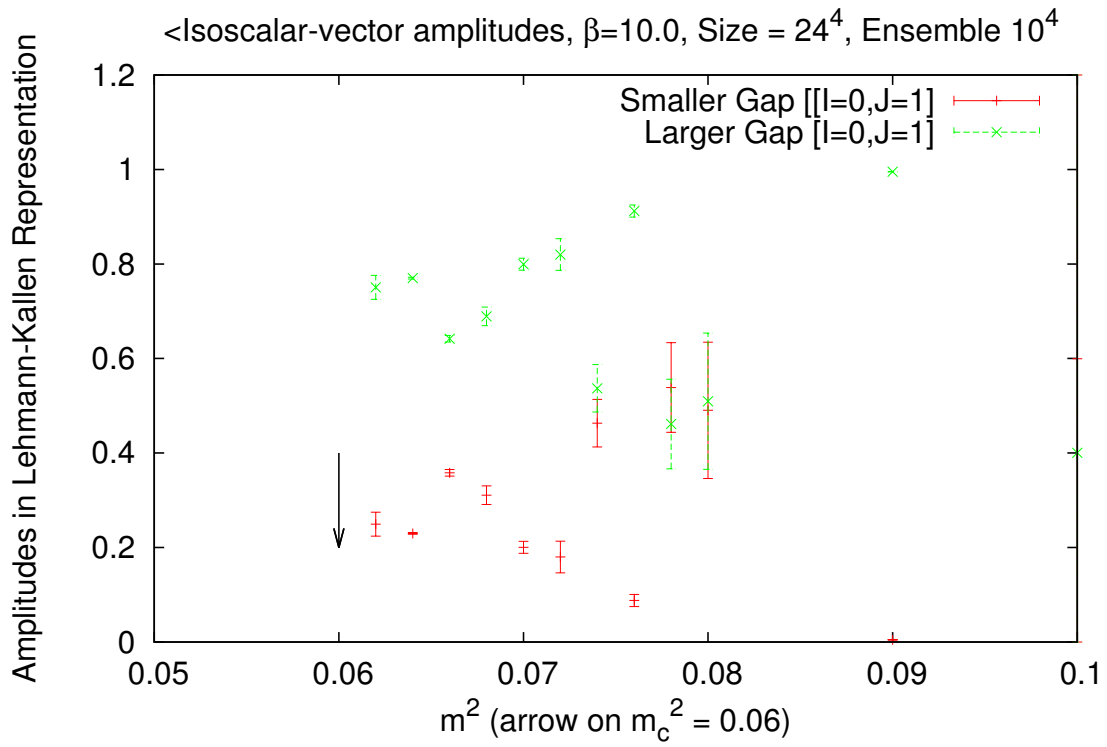


Figure 11: Weights in the isoscalar channel ($J = 1$) for $\beta = 10$.